Effects of Matrix Temperature and Rigidity on the Electronic Properties of Solvatochromic Molecules: Electroabsorption of Coumarin 153

Arindam Chowdhury, Sarah A. Locknar, Lavanya L. Premvardhan, and Linda A. Peteanu*

Department of Chemistry, Carnegie Mellon University, Pittsburgh, Pennsylvania 15213

Received: July 23, 1999; In Final Form: September 29, 1999

Using Stark effect (electroabsorption) spectroscopy to study the well-known solvatochromic probe molecule coumarin 153 (C153) in a variety of polymer matrices and organic glasses, we have found that the average change in polarizability ($\overline{\Delta\underline{\underline{\alpha}}}$) that we measure depends critically on the rigidity of the matrix used. In rigid polymer and frozen organic glass matrices, the measured values $\overline{\Delta\underline{\underline{\alpha}}}$ are between 4 and 60 Å^3. The smaller values in this range are similar to those obtained via semiempirical and ab initio calculations. In contrast, measurements made on polymer matrices that are above their glass-transition temperature or those containing trapped solvent are more than an order of magnitude higher. We postulate that large values of $\overline{\Delta\underline{\underline{\alpha}}}$ result from field-induced orientation of the C153 molecule and/or the dipoles of the surrounding matrix in matrices that are not fully rigid. The absolute value of the change in dipole moment between the ground and excited states ($|\Delta\underline{\mu}|$) of C153 measured here ranges from 4.4 to 7.0 D, depending on the polarity and the rigidity of the environment. In addition, an apparent local enhancement of the polarity of the cavity containing C153 is observed in both the solvent and polymer glass matrices, as inferred by the absorption maximum of C153 in these environments.

Introduction

Coumarin 153 (C153), shown in Figure 1, is a frequently used fluorescent probe for the static and dynamic aspects of solvation because the wavelength maxima of its absorption and emission bands are very sensitive to the polarity of the molecular environment. C153 is a polar molecule with a large ground-state dipole moment (6.55 D).[1] Values of the difference dipole moment between the ground and excited states, $\Delta\underline{\mu}$, of between 4 and 9 D have been reported in various solvents through electrooptic studies,[2] transient dc photocurrent experiments,[3] and solvatochromic measurements.[4−7] In addition, a number of calculations at the semiempirical[4,6,8,9] and ab initio levels for $\Delta\underline{\mu}$ are available.[10] Interest in accurate measurements and calculations of the $\Delta\underline{\mu}$ of C153 and other coumarins stems from the importance of this quantity to modeling of the solvation dynamics of these molecules and to prediction of the values of their nonlinear optical coefficients (β).[1,11] Table 1 contains a summary of the available experimental and theoretical data on the $\Delta\underline{\mu}$ of C153.

While measurements of $\Delta\underline{\mu}$ have received considerable attention in the literature, none of the published accounts report a value for the average change in polarizability on excitation ($\overline{\Delta\underline{\underline{\alpha}}}$). In the past few years, however, a number of recently published theoretical papers have suggested that electronic polarizability makes a substantial contribution to the solvation response even of polar solutes such as C153. For example, studies by Marcus,[7] Maroncelli,[12] Ando,[13] Rempel,[9] Callis,[14] and their respective co-workers have examined the importance of the polarizability of a solute in modeling its static and dynamic Stokes shift behavior and the spectral line width of its emission. Bursulaya and Kim have demonstrated effects due to solute ground- and excited-state polarizabilities on photon-echo measurements[15] and on the overall solvation dynamics and emission line width of a model solute.[16,17] More recently, Matyushov and Voth have predicted a substantial effect on the line shape of the absorption and emission spectra of a chromophore due to the difference in polarizabilities of the ground and excited states.[18]

One of most frequently used methods to measure $\overline{\Delta\underline{\underline{\alpha}}}$ and $|\Delta\underline{\mu}|$ is Stark spectroscopy.[19,20] This technique involves the application of an external electric field to a fixed isotropic sample of molecules in a host matrix. Interaction between the

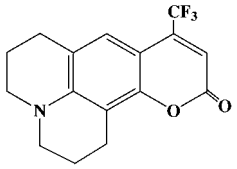

Figure 1. Coumarin 153.

TABLE 1: Values of $\Delta\underline{\mu}$ for C153

method[a]	$\Delta\underline{\mu}$ (D)
AM1 HF/SCI[b]	6.96
AM1 HF/SCI[c]	7.5 ($\theta = 10°$)[a]
MNDO HF/SCI[d]	7.9
ab initio HF/SCI[e] (3-21G)	4.88 ($\theta = 6°$)
ab initio HF/SCI[f] (6-21G*)	3.8 ($\theta = 7°$)
Stokes Shift[g]	6.4[h] ($\theta = 10°$), 4.23[i]
Stokes Shift[j]	4.1,[k] 7.5[l]
electrooptic (solution)[m]	7.3−9.6
transient dc photocurrent[n]	8.5−9.5

[a] Calculations (first five entries) are gas-phase. Experiments (remaining entries) are as reported in the corresponding references. θ is the angle between $\underline{\mu}_e$ and $\underline{\mu}_g$ and assumed to be zero unless noted. [b] Reference 8. [c] Reference 6. [d] Reference 12. [e] This work. [f] Reference 10. [g] Reference 6. [h] Lipperts method. [i] Ratio method. [j] Reference 4.[k] For a cavity radius of 3.9 Å. [l] For a cavity radius of 5.85 Å. [m] Reference 2. [n] Reference 3.

* To whom correspondence should be addressed. E-mail: peteanu@andrew.cmu.edu.

10.1021/jp992567b CCC: $18.00
Published on Web 11/05/1999

applied field and the molecular dipoles creates a broadening or splitting of the absorption spectrum that is proportional to $|\Delta\underline{\mu}|$, which is the absolute value of the vector difference between the vectors $\underline{\mu}_e$ and $\underline{\mu}_g$. In addition, a field-induced *shift* of the spectrum (usually to lower energy) is attributed to the change in polarizability between the ground and excited electronic states of the molecule. While these two effects generally dominate the molecular response in Stark spectroscopy, symmetry breaking and other field effects on transition moments have also been reported in the literature.[19]

In previous work on polar polyenes (retinals) in polymethyl methacrylate (PMMA) at room temperature, we noted a large discrepancy between the change in polarizability on excitation measured using Stark spectroscopy ($\overline{\overline{\Delta\alpha}}^{Stark}$) and the $\overline{\overline{\Delta\alpha}}$ that is calculated via semiempirical methods.[21] The calculated value represents the electronic $\overline{\overline{\Delta\alpha}}$, which we designate as $\overline{\overline{\Delta\alpha}}^{el}$. In several instances, the values of $\overline{\overline{\Delta\alpha}}^{Stark}$ measured were 4−5 times larger than calculations of the corresponding quantities. In contrast, we found far better agreement between experiment and calculation in the case of the nonpolar diphenylpolyenes.[22] This marked difference in the results for the polar and nonpolar systems suggested the possibility that the field-induced orientation of the probe molecule and/or of polar groups in the matrix may make a substantial contribution to the value of $\overline{\overline{\Delta\alpha}}^{Stark}$. This is an *orientational* contribution to $\overline{\overline{\Delta\alpha}}^{Stark}$ that is over and above the $\overline{\overline{\Delta\alpha}}^{el}$ of the molecule, which is also the quantity that is calculated. The relationship between these terms is defined explicitly in Experimental Section below.

Support for this interpretation of the electroabsorption results comes from the strong dependence of the $\overline{\overline{\Delta\alpha}}^{Stark}$ of the retinals on both the rigidity and the temperature of the matrix used.[23] In contrast, the polarity effect on $\overline{\overline{\Delta\alpha}}^{Stark}$ was found to be relatively *weak*. In this work, we reexamine the role of the polarity and rigidity of the matrix as well as accuracy of the finite-field method of calculating excited-state polarizabilities for the solvatochromic probe molecule C153.

There are a number of simplifications afforded by the choice of C153 rather than retinal as a probe. Like retinals, C153 is polar.[1] However, *unlike* retinals, C153 is structurally rigid (Figure 1). Therefore, we expect to minimize the possibility of effects due to polarity-induced changes in conformation such as have been observed for retinals.[24] Moreover, in substituted linear polyenes, the linear and higher order polarizabilities may be significantly altered because of changes in the C═C and C−C bond lengths with an applied electric field or the solvent field.[25] In contrast, no significant changes in molecular structure with solvent polarity are expected for C153. Finally, predicting the polarity response of retinals is complicated by the fact that these molecules have two closely lying excited electronic states, the optically allowed $1B_u$ state and the nominally forbidden $2A_g$ state,[26] whose relative energies depend on solvent polarity.[27] In contrast, there is some supporting evidence in the literature[28] that the absorption band of C153 consists of a $\pi-\pi^*$ excitation to an electronic state that is well-separated energetically from other singlet excited states. The validity of this picture shall be one of the subjects addressed in this work.

The electroabsorption data presented here are for C153 in a variety of polymer matrices and organic solvent glasses that are all commonly used for Stark spectroscopy. We chose polyethylene (PE), polymethyl methacrylate (PMMA), and poly(vinyl chloride) (PVC) as our polymer matrices and 2-methyltetrahydrofuran (MeTHF) and toluene as solvents to form frozen glasses containing the C153 molecules. Measurements of the polymer systems were performed at two temperatures, 298 and 77 K. At room temperature, the pristine forms of two of the polymers (PMMA and PVC) are below their glass-transition temperatures (T_g), while PE is below its T_g only at the lower temperature. In addition, PE is less polar than either PMMA or PVC, the last two being of similar polarity. The organic glasses were also chosen to have somewhat different polarities in order to determine the effects of this parameter on the measured properties of C153.

The data obtained show, in agreement with our previous work on all-trans retinal, that field-induced orientations manifest themselves in a contribution to $\overline{\overline{\Delta\alpha}}^{Stark}$ that is highly dependent on both the temperature and the rigidity of the matrix.[23] When the available thermal energy is minimized and an organic solvent that forms a rigid glass is used as the matrix, the measured and calculated values of $\overline{\overline{\Delta\alpha}}$ agree, both being relatively small ($\sim$10 Å^3). Again, the polarity effect on $|\Delta\underline{\mu}|$ is small, consistent with a small induced moment and therefore a small $\overline{\overline{\Delta\alpha}}^{el}$. Because we find that the measured $\overline{\overline{\Delta\alpha}}^{Stark}$ of a molecule is extremely sensitive to the rigidity of the local environment, electroabsorption spectroscopy is an effective probe of molecular motions even within matrices that are below their respective T_g's. Such reorientations are related to the ability of applied fields to induce ordering of molecular dipoles in a matrix, such as for photorefractive applications or for second-harmonic generation, as well as to the decay in such ordering that is observed over time.

A useful feature of C153 is that the wavelength of its absorption maximum provides a measure of the local polarity of its environment. This is important because, in the matrices studied here, there is evidence that the polarity of the environment local to the dopant molecule may not be well described by the bulk dielectric constant of the matrix. This has been demonstrated in the case of organic solvent glasses. The presence of a polar molecule within these glasses causes an enhancement of the local matrix polarity upon freezing.[29] Here, we find evidence of a similar polarity enhancement, this time for C153 in polymers that form glasses at room temperature. The important consequences of this internal field enhancement for measurements of molecular hyperpolarizabilities, at least for molecules in organic solvents and their glasses, have been previously demonstrated.[30] Since high-T_g polymeric films such as PMMA are frequently used for fabricating nonlinear optical devices, the observation that the local polarity of the environment of dopant molecules is *also* enhanced in those media is of significance from the standpoint of applications.

Experimental Section

Materials. C153, polymethyl methacrylate (PMMA), poly(vinyl chloride) (PVC), and dichloroethane (all from Aldrich) were used without further purification. Toluene (Fisher), MeTHF (Acros), and methylcyclohexane (MCH; Aldrich) were used immediately after refluxing under Ar atmosphere over CaH_2 for at least an hour to remove water.

Sample Preparation. Polymer films of PMMA and PVC were prepared by dissolving the molecule of interest and the desired polymer together in dichloroethane, pouring the mixture into an aluminum dish and evaporating the solvent. PMMA films were then either glued between ITO (indium tin oxide)-coated slides with a viscous solution of PMMA in dichloroethane and left to dry for 24 h (glued PMMA) or were clamped between the slides, heated in an oven at 150 °C for 5 min, and then used immediately (heated PMMA). The latter method exclusively was used for the preparation of PVC films. PE films were prepared by swelling the films in a chloroform solution

containing the molecule of interest at millimolar concentration. After at least 10 min, the films were removed, washed with methanol, allowed to air-dry, and heated between two inconel slides (Melles Griot) as described above. The organic glasses were prepared with C153 dissolved in dried solvents such that the final absorbance of the sample was 0.2−0.8. The solution was placed within a well created with Kapton tape (~50 μm thick) that was applied to an ITO-coated glass slide. Another ITO-coated slide was pressed onto the first and held in place with spring clips. The entire sample cell was then immersed in a liquid nitrogen optical Dewar (H. S. Martin).

To obtain an accurate measure of the film and cell thicknesses, an interference pattern of fringes was measured in the 900−2500 nm range using a UV−vis−NIR absorption spectrometer (Perkin-Elmer Lambda 900) as described previously.[21] This interference method gave a standard deviation in the thickness of 2 μm.

We tested for aggregation of the C153 molecules in the various environments used in the following ways. The absorption spectra of C153 obtained in the frozen organic glasses were compared with those in the corresponding room-temperature solutions (at micromolar concentration) and found to contain no new features that would indicate the formation of aggregates. The absorption spectra in the polymer samples were compared to those obtained at micromolar concentration in room-temperature solvents of comparable polarities. Again, both were found to contain the same features. One matrix that we tried, methylcyclohexane glass, *did* cause C153 to aggregate as shown both by the appearance of additional peaks in the absorption spectrum and by the poor fit to the electroabsorption spectrum that was obtained as a consequence. Therefore, the data for C153 in methylcyclohexane are not reported here. In contrast, the absorption spectrum of C153 in PE, another low-dielectric medium used in this work, is of normal appearance and the fit to the electroabsorption spectrum is of high quality.

Theory of Electroabsorption and Data Analysis Procedures. The theory behind electroabsorption was developed by Liptay[31] and is summarized here with some slight changes in formalism. The overall change in transmitted light intensity caused by the application of an electric field is described by the following equation:

$$\left(\frac{2\sqrt{2}}{2.303}\right)\frac{\Delta I}{I} = \underline{\epsilon}^2\left[a_\chi A(\nu) + b_\chi \frac{\nu}{h}\frac{\partial}{\partial\nu}\left(\frac{A(\nu)}{\nu}\right) + c_\chi \frac{\nu}{h^2}\frac{\partial^2}{\partial\nu^2}\left(\frac{A(\nu)}{\nu}\right)\right] \quad (1)$$

The $\Delta I/I$ term is a measure of the intensity change as a result of the applied field (ΔI) normalized to the total light intensity reaching the detector (I). The unperturbed absorption spectrum is designated $A(\nu)$. Both ΔI and I were measured simultaneously by the lock-in amplifier, using the locked (ΔI) and total voltage (I) channels. The factor of $2\sqrt{2}$ is needed to convert from rms voltage (read in by the lock-in amplifier) to an equivalent dc voltage, and the factor of 2.303 is derived from treating the field-induced intensity change as a perturbation to the intensity. The $A(\nu)$ represents the unperturbed absorption as a function of frequency, and $\underline{\epsilon}$ represents the field at the sample in V/cm. This effective field includes the enhancement of the applied field due to the cavity field of the matrix. The subscript χ represents the angle between the direction of the applied electric field and the electric field vector of the polarized light as shown in Figure 2. The expressions for a_χ, b_χ, and c_χ are given below for the magic angle ($\chi = 54.7°$).

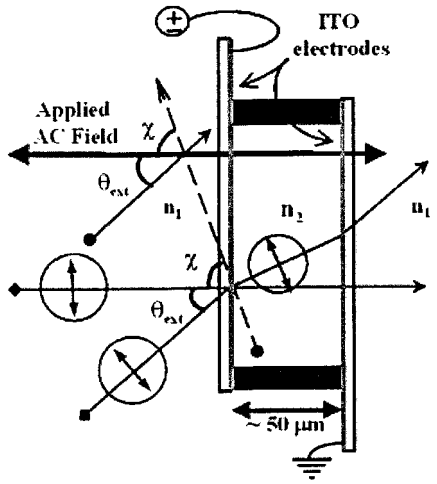

Figure 2. Horizontal cross section of the sample cell. The double-headed arrows in the circles represent the polarization of light. The bold double-headed arrow shows the direction of the applied electric field. θ_{ext} is the angle between the direction of propogation of the light beam and the direction of the applied electric field. χ is the angle between the direction of polarization of light after refraction and the direction of the applied electric field. The refractive indices of the external medium (air or liquid nitrogen) and the sample glass are n_1 and n_2, respectively.

$$a_{54.7} = \frac{1}{3|\underline{m}|^2}\sum_{i,j} A_{ij}^{\ 2} + \frac{2}{3|\underline{m}|^2}\sum_{i,j} m_i B_{ijj} + \frac{2\beta}{3|\underline{m}|^2}\sum_{i,j} m_i A_{ij}\mu_{gj} \quad (2)$$

$$b_{54.7} = \frac{2}{3|\underline{m}|^2}\sum_{i,j} m_i A_{ij}\Delta\mu_j + \frac{1}{2}\overline{\underline{\underline{\Delta\alpha}}}^{el} + \frac{\beta}{3}(\underline{\mu}_g \cdot \Delta\underline{\mu}) \quad (3)$$

$$c_{54.7} = \frac{1}{6}|\Delta\underline{\mu}|^2 \quad (4)$$

The symbols α and μ represent the polarizability and dipole moment, respectively. A bar above a quantity indicates its average value (i.e., $\overline{\underline{\underline{\Delta\alpha}}} = (1/3)\mathrm{Tr}(\underline{\underline{\Delta\alpha}})$), a single bar below a quantity designates a vector, and a double bar denotes a tensor. The indices i and j label the vector/tensor components along x, y, and z. The transition moment is represented by $\underline{m}$, and the tensors $\underline{A}$ and $\underline{\underline{B}}$ represent the transition polarizability and hyperpolarizability, respectively. These describe the effect of $\underline{\epsilon}$ on the molecular transition moment: $\underline{m}(\underline{\epsilon}) = \underline{m} + \underline{A}\cdot\underline{\epsilon} + \underline{\epsilon}\cdot\underline{\underline{B}}\cdot\underline{\epsilon}$. Because one of the focuses of this paper is on measurements of the $\overline{\underline{\underline{\Delta\alpha}}}^{el}$ of C153, we will discuss the terms in eq 3 in some detail. Note that the fit to the experimental electroabsorption spectrum gives $b_{54.7}$, which we identify as the measured value $\overline{\underline{\underline{\Delta\alpha}}}^{Stark}$ in this work. To equate $\overline{\underline{\underline{\Delta\alpha}}}^{Stark}$ with $\overline{\underline{\underline{\Delta\alpha}}}^{el}$ alone (eq 3), we must make two assumptions. One is to neglect the transition moment polarizability, thereby eliminating the first term. Strictly speaking, the transition moment polarizability is a higher-order correction to $\overline{\underline{\underline{\Delta\alpha}}}^{el}$. Neglect of this term is justifiable because sizable field effects on transition moments are normally seen only in forbidden transitions, not in strongly allowed $\pi-\pi^*$ transitions, such as that of C153.[32,33] Moreover, further evidence that the effect of the applied field on the transition moment is small is found in the work of Lewis and Maroncelli, whose study of the magnitude of the extinction coefficient of C153 as a function of solvent polarity failed to reveal a significant variation.[28] The second assumption we must make is to neglect the term containing the Boltzman prefactor, $\beta = 1/(kT)$. This term arises in Liptay's formation for the field-induced molecular orientation to first order. Neglect of this term is valid if the C153 molecules are isotropically distributed in a rigid environ-

TABLE 2: Electroabsorption Results for C153 in Various Matrices and Different Temperatures [a]

						$f^2\cdot\overline{\Delta\underline{\underline{\alpha}}}_{calc}$[d]			$f\cdot\Delta\underline{\mu}_{calc}$[d]	
matrix	T_g[b]	ϵ_0	n_2	λ_{max}[c]	$\overline{\Delta\underline{\underline{\alpha}}}^{Stark}$	3-21G	6−21G*	$\lvert\Delta\underline{\mu}\rvert$	3-21G	6-21G*
PE (298 K)	148	2.3	1.51	396	374(3)	6.62	6.87	4.4(0.3)	6.23	5.01
PE (77 K)	148	2.3	1.58	397	26(7)	6.62	6.87	5.3(0.2)	6.23	5.01
PMMA[e]		10.7	1.44	418	564(80)			5.7(0.6)		
PMMA[f]	378	3.6	1.49	418	60(3)	7.54	7.88	5.6(0.1)	6.70	5.42
PVC[g]	354	3.5	1.55	426	46(3)	7.50	7.83	5.3(0.1)	6.68	5.40
toluene[h]	119	2.6[i]	1.5[i]	418	6(1)	6.89	7.70	5.8(0.4)	6.37	5.13
MeTHF[h]	91	5.4[i]	1.41[i]	418	4(2)	8.15	8.57	7.0(0.4)	7.00	5.68
		19[j]	1.73[j]			9.27	9.82		7.56	6.16

[a] Polarizabilities in Å^3 and dipole moments in debye. [b] In kelvin.[40,42,62] [c] In nanometers. [d] Calculated values have been scaled by both cavity and reaction fields for an oblate spheroid. The first column shows results of 3-21G calculations on a 6-31G optimized structure. The second column shows results of 6-21G* calculations. [e] Glued PMMA. [f] Heated PMMA. [g] Measurements at 298 K. [h] Measurements at 77 K. [i] 298 K parameters.[62] [j] 94 K parameters.[40]

ment and therefore cannot reorient on the time scale of the oscillating applied electric field. In essence, a fixed, isotropic distribution corresponds to a very high temperature ($\beta \approx 0$), *regardless* of the actual temperature of the sample because the molecular dipoles remain random even in the presence of an aligning field. One focus of this paper is to determine whether this approximation is valid for polar molecules in polymer and organic frozen glasses.

Information regarding $|\Delta\underline{\mu}|$ for the molecule is contained in the $c_{54.7}$ term (eq 4). If the orientation of the dipoles of the molecules in the matrix is isotropic and fixed, there will be an equal number of molecules oriented parallel and antiparallel to the applied field at all times. These molecules will be stabilized or destabilized, respectively, to an equal extent by the applied field. An overall broadening of the absorption spectrum will result if the excited-state dipole moment is different from that of the ground state. This field-induced broadening gives rise to a contribution to the electroabsorption spectrum that is proportional to the second derivative of the unperturbed absorption spectrum. Though some effect on the magnitude of $c_{54.7}$ due to orientation of the probe molecule is apparent in our results, it is much smaller than observed for $b_{54.7}$ (vide infra). Our reported values for $|\Delta\underline{\mu}|$ are therefore always those obtained directly from application of eq 4. For a more detailed discussion of these effects, see refs 20 and 31.

Instrumentation. Electroabsorption spectra were obtained with a home-built spectrometer that has been described previously.[21] In essence, it consists of a 150 W xenon arc lamp (Oriel), single 0.3 m monochromator (Spex), horizontal polarizer, and photodiode detector (UDT), which is connected to a lock-in amplifier (Stanford Research SR850). A high-voltage ac power supply (Joe Rolfe) is used to deliver 10^5-10^6 V/cm to the sample via optically transparent electrodes at a frequency of ~450 Hz. The power supply also provides the reference frequency for the phase-sensitive light detection in the lock-in amplifier. Figure 2 shows the sample cell in detail. The external angle (θ_{ext}) is defined as the angle between the direction of propagation of light *outside the sample cell* and the direction of the electric field vector of the applied ac field. In this case, the vector of the applied field is always normal to the sample cell surface. The angle χ is that between the direction of polarization of the electric field vector of the incident photon (horizontally polarized) *inside the sample cell* and the direction of the electric field vector of the applied ac field. By this definition, $\chi = 90°$ for $\theta_{ext} = 0°$. To change the angle χ from 90° to 54.7°, we rotate the sample holder relative to the direction of propagation of the light beam. To determine[20] by what angle θ_{ext} we must rotate the sample in order to obtain a value of χ *o*f 54.7°, we use Snell's law. Applying Snell's law of refraction, one can readily see from Figure 2 that

$$n_1 \sin(\theta_{ext}) = n_2 \sin(90 - \chi)$$

and hence

$$\theta_{ext} = \sin^{-1}\left[\frac{n_2}{n_1}\cos(\chi)\right]$$

where n_1 = refractive index of air (1.00) or liquid nitrogen (1.2), whichever is appropriate, and n_2 = refractive index of the sample. For instance, in order to have $\chi = 54.7°$ for the polymer samples ($n_2 = 1.5$), we must set θ_{ext} to 60° when air is the external medium and 46° for liquid nitrogen.

Electronic Structure Calculations. The geometry of C153 was optimized with a 6-31G basis set using Hartree−Fock (HF) theory within the Gaussian 94 package of programs.[34] Ground-state properties were determined from SCF calculations using HF/3-21G. The excited state was modeled using singles configuration interaction (CI) with a 3-21G basis set. Using these methods, we have obtained gas-phase values of $\underline{\mu}_g$ (6.97 D) and $\underline{\mu}_e$ (11.76 D) that yield a gas-phase calculated value for $\Delta\underline{\mu}$ of 4.88 D. Here, the vectorial difference was taken because the calculated angle between $\underline{\mu}_g$ and $\underline{\mu}_e$ is 6°. The gas-phase value of $\Delta\underline{\mu}$ obtained at the 3-21G level is ~28% larger than that obtained using a 6-21G* basis set ($\Delta\underline{\mu}$ = 3.8 D).[10] The polarizabilities were calculated using a finite-field method coupled to the HF calculation for the ground state and the CI calculation for the excited state. We calculated a gas-phase value of $\overline{\Delta\underline{\underline{\alpha}}}^{el}$ of 4.4 Å^3, while a value of 4.33 Å^3 was obtained at the 6-21G* level.[10] For the calculation of $\overline{\Delta\underline{\underline{\alpha}}}^{el}$, finite-field methods have been shown by us[22] and others[35] to give accurate values in a variety of chemical systems. The ab initio finite-field results are lower than the results of the INDO/MRD/SDCI method[36] (12.4 Å^3),[37] which uses the sum-over-states formalism. However, prior to this work, there have been no experimental results for $\overline{\Delta\underline{\underline{\alpha}}}$ for C153 with which a comparison with calculation could be made.

For the calculated values of $\Delta\underline{\mu}$ and $\overline{\Delta\underline{\underline{\alpha}}}^{el}$ reported in Table 2, we have included both the results obtained at the 3-21G level (left side) and 6-21G* (right side). To facilitate comparison with experimental results, all of the gas-phase calculations that are reported in Table 2 were corrected for solvation. These values are referred to in Table 2 as $f\cdot\Delta\underline{\mu}_{calc}$ and $f^2\cdot\overline{\Delta\underline{\underline{\alpha}}}_{calc.}$ This was done as described previously[38] using both Onsager-type reaction fields and cavity fields,[31] modified for an ellipsoidal cavity.[39] The dimensions of the ellipsoidal cavity are 6.1 Å for the major semiaxes and 2.3 Å for the minor semiaxis, yielding an overall volume of 359 Å^3. With the exception of MeTHF, the dielectric

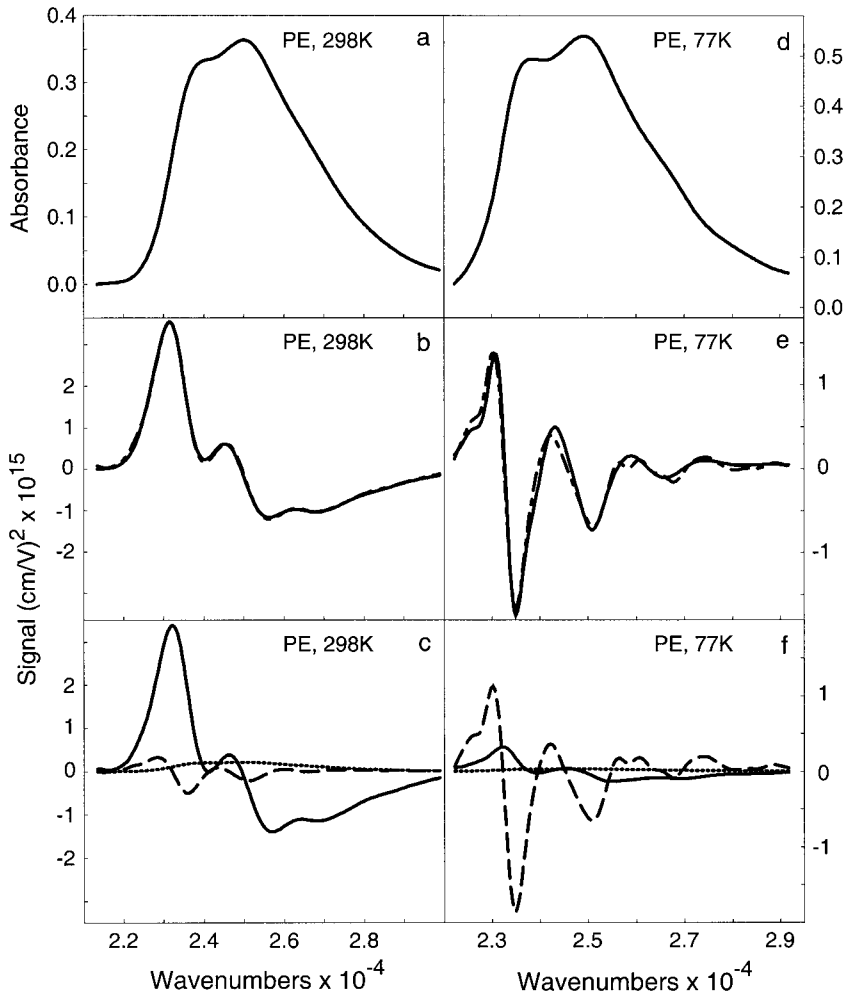

Figure 3. C153 in a PE matrix at 298 K (a−c) and 77K (d−f). The first panel shows the absorption spectrum at 298 K (a) and at 77 K (d). The second panel shows the electroabsorption (solid) and fit (dashed−dot) for $\chi = 54.7°$ at 298 K (b) and 77 K (e), respectively. The third panel shows the individual components of the fit to the electroabsorption signal at 298 K (c) and 77 K (f). The absorption spectrum (dotted), first derivative of the absorption spectrum (solid), and the second derivative of the absorption spectrum (dashed), all normalized to the applied field, are shown.

constants and refractive indices used (Table 2) are bulk values that may not necessarily reflect the dielectric behavior at the site of the C153 molecule (vide infra). Recent work by Richert suggests that the dielectric constant of MeTHF near 77 K is 19.[40] Therefore, we have performed reaction-field and cavity-field corrections on the gas-phase calculated numbers using both the room-temperature and low-temperature dielectric constants of MeTHF that are shown in Table 2.

Results and Discussion

In the following sections, we will first discuss the predictions of ab initio and semiempirical calculations of the quantities $|\Delta\underline{\mu}|$ and $\overline{\Delta\underline{\underline{\alpha}}}^{el}$ of C153 as well as prior measurements of $|\Delta\underline{\mu}|$ made utilizing electroabsorption, transient photocurrent, and solvatochromic methods. Next, we will detail the results of electroabsorption measurements performed on C153 in a variety of polymers and organic solvent glasses as described in Introduction. The initial focus will be on a comparison between our measured values of $|\Delta\underline{\mu}|$ and those in the literature. Following this, the observed variation of the measured $\overline{\Delta\underline{\underline{\alpha}}}^{Stark}$ with the temperature and the matrix used will be rationalized in terms of an orientational model. Finally, the electroabsorption results are used to examine the proposal, which has been put forth in the literature, that more than one electronic excited state underlies the main absorption band of C153.[41]

Theoretical Predictions for $|\Delta\underline{\mu}|$. Both of the ab initio results described above for $\Delta\underline{\mu}$ are significantly smaller than published results obtained by semiempirical methods (gas-phase values summarized in Table 1). Correction of both sets of ab initio results for enhancement due to the cavity and reaction fields brings them within the range reported from solvatochromic studies and from prior electroabsorption experiments on C153 in room-temperature solvents (Table 1). However, there is substantially better agreement between our experimental results for $|\Delta\underline{\mu}|$ (Table 2) and the calculated results obtained using the 6-21G* basis set, [10] as can be seen by comparison of the second set of numbers in the column headed $f\cdot\Delta\underline{\mu}_{calc}$ with experiment ($|\Delta\underline{\mu}|$). Note that the calculations in Table 2 predict that *neither* $|\Delta\underline{\mu}|$ nor $\overline{\Delta\underline{\underline{\alpha}}}$ will vary significantly as the dielectric constant of the medium is changed over a fairly wide range. This is in accord with the published results of Stark measurements in solution phase. Baumann and Nagy found that the $|\Delta\underline{\mu}|$ of C153 is essentially constant as the solvent dielectric constant varies from that of cyclohexane ($\epsilon_0 = 2.02$) to that of benzotrifluoride ($\epsilon_0 = 9.04$).[2] Nevertheless, we will show below that measurements of $\overline{\Delta\underline{\underline{\alpha}}}^{Stark}$ vary by *over nearly 2 orders of magnitude* depending on the matrix chosen and on its temperature. Some variation in $|\Delta\underline{\mu}|$ is also seen though it is far less dramatic.

Electroabsorption of C153 in Polymer Films. The electroabsorption spectrum of C153 in PE is shown in Figure 3. The

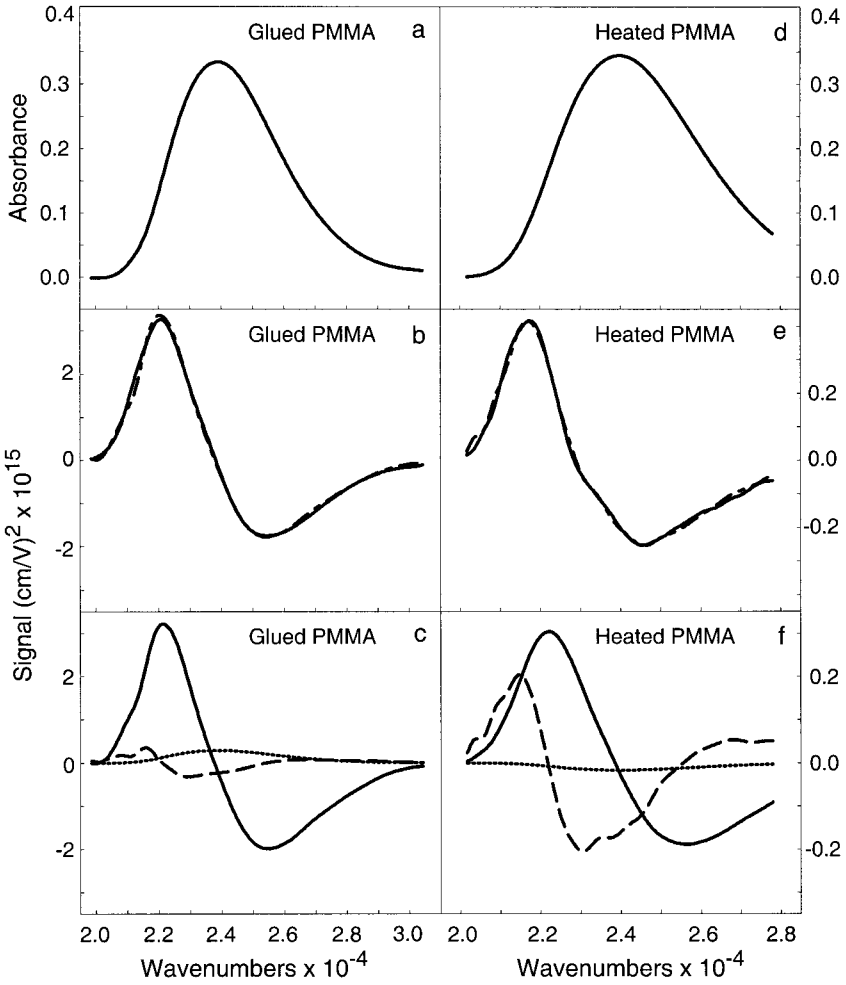

Figure 4. C153 in a glued (a−c) and a heated (d−f) PMMA matrix at 298 K. The first panel shows the absorption spectrum of the glued (a) and the heated (d) samples. The second panel shows the electroabsorption (solid) and fit (dashed−dot) for $\chi = 54.7°$ of the glued (b) and the heated (e) samples, respectively. The third panel shows the individual components of the fit to the electroabsorption signal of the glued (c) and the heated (f) samples. The absorption spectrum (dotted), first derivative of the absorption spectrum (solid), and the second derivative of the absorption spectrum (dashed), all normalized to the applied field, are shown.

upper, middle, and lower panels show the absorption, electroabsorption (solid) and fit (dashed−dot), and the weighted individual components of the fit to the electroabsorption signal of C153 at $\chi = 54.7°$. The left and right columns show the spectra obtained at 298 and at 77 K, respectively. The Stark spectrum at 77 K is more structured (Figure 3b) than that at room temperature (Figure 3e). In addition, the electroabsorption spectrum at 298 K contains a substantial contribution from a first-derivative line shape (Figure 3b), while that at 77 K is clearly dominated by the second-derivative component (Figure 3e). This is also indicated by the relative magnitudes of the individual components of the fits to the electroabsorption signal (compare Figure 3c to Figure 3f). As described in Experimental Section, the contribution of the first-derivative component is proportional to $\overline{\Delta\underline{\underline{\alpha}}}^{\text{Stark}}$ while that of the second-derivative component is proportional to $|\Delta\underline{\mu}|$.[2] The results for $|\Delta\underline{\mu}|$ and $\overline{\Delta\underline{\underline{\alpha}}}^{\text{Stark}}$ for C153 in PE are summarized in Table 2.

Figure 4 contains the electroabsorption spectrum of C153 in PMMA at 298 K for $\chi = 54.7°$. As before, the three panels (top to bottom) show the absorption, electroabsorption (solid) and fit (dashed−dot), and the weighted individual components of the fit to the electroabsorption spectrum. The left column contains the spectra of C153 in glued PMMA, while the right column contains those of C153 in heated PMMA (see Experimental Section). The heated sample gives rise to a slightly more structured Stark spectrum than that of the glued sample. Considering the individual components to the fit, the glued sample has a first-derivative contribution that is ∼10 times larger than that of the heated sample. (Figure 4c,f, solid line). Consequently, the $\overline{\Delta\underline{\underline{\alpha}}}^{\text{Stark}}$ obtained for the glued samples is an order of magnitude larger than that for the heated samples (Table 2).

Interestingly, we find that at room temperature the magnitudes of $\overline{\Delta\underline{\underline{\alpha}}}^{\text{Stark}}$ for C153 in the heated polymer glass samples (PMMA and PVC) *still* exceed the calculated values by up to an order of magnitude. To determine whether this is due to residual thermal motion of the chromophore within the matrix, we compared the electroabsorption spectra of PVC ($T_g = 354$ K) at room temperature and in liquid nitrogen (Figure 5). The contributions of the individual components of the fit to the Stark spectrum for PVC at 298 and at 77 K are shown in panels c and f. The first-derivative component (solid line) is indeed substantially diminished at 77 K relative to that at 298 K, correlating to a decrease in $\overline{\Delta\underline{\underline{\alpha}}}^{\text{Stark}}$ as the temperature of the matrix is lowered. We postulate that the lowering of $\overline{\Delta\underline{\underline{\alpha}}}^{\text{Stark}}$ occurs because contributions arising from molecular reorientation (third term, eq 3) are minimized as the matrix is made more rigid. Again, as this term approaches zero, $\overline{\Delta\underline{\underline{\alpha}}}^{\text{Stark}}$ will approach $\overline{\Delta\underline{\underline{\alpha}}}^{\text{el}}$ if the transition moment polarizability is also small.

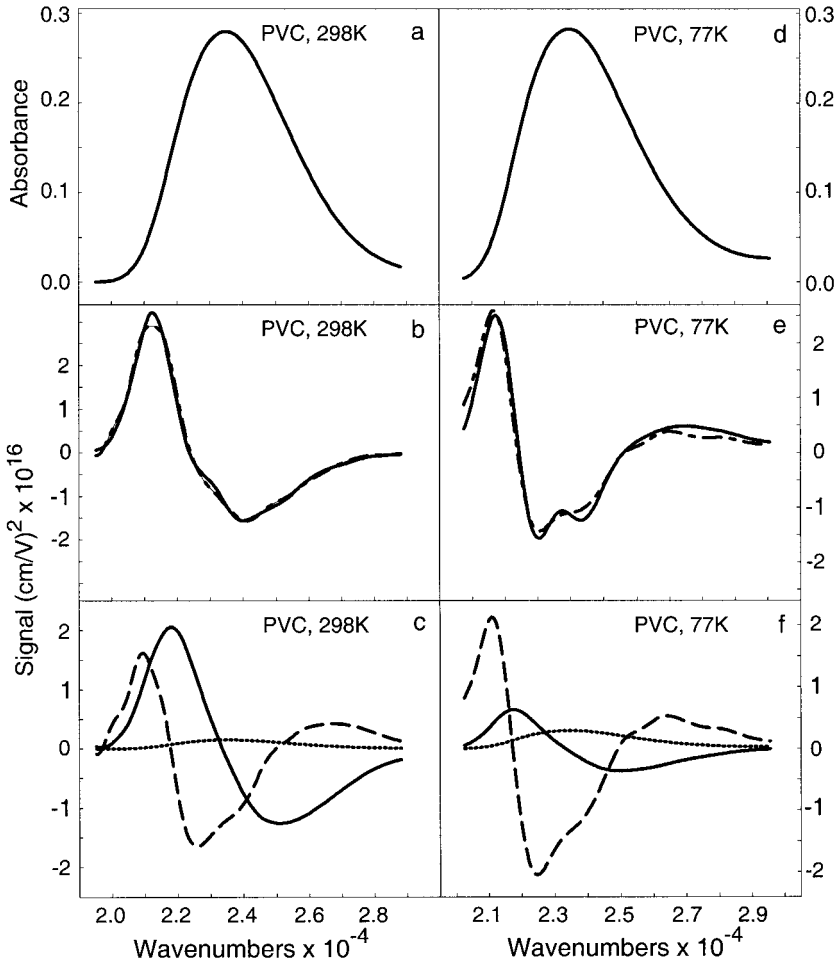

Figure 5. C153 in a PVC matrix (heated) at 298 K (a−c) and 77 K (d−f). The first panel shows the absorption spectrum at 298 K (a) and at 77 K (d). The second panel shows the electroabsorption (solid) and fit (dashed−dot) for $\chi = 54.7°$ at 298 K (b) and 77K (e), respectively. The third panel shows the individual components of the fit to the electroabsorption signal at 298 K (c) and 77 K (f). The absorption spectrum (dotted), first derivative of the absorption spectrum (solid), and the second derivative of the absorption spectrum (dashed), all normalized to the applied field, are shown.

Electroabsorption Spectra in Organic Solvent Glasses. To compare our measurements of $\overline{\Delta\underline{\underline{\alpha}}}^{\text{Stark}}$ in polymer matrices to those obtained in small organic solvent glasses, we performed electroabsorption measurements on C153 in frozen toluene and MeTHF. Both form optically clear glasses in liquid nitrogen, their T_g's being 119 and 91 K, respectively.[40,42] Figure 6 contains the electroabsorption spectrum of C153 in toluene (left) and MeTHF (right) at 77 K for $\chi = 54.7°$. As before, the three panels show the absorption, electroabsorption (solid) and fit (dashed−dot), and the weighted individual components of the fit to the electroabsorption signal. The Stark spectra of this molecule in the solvent glasses are clearly dominated by the second-derivative line shape as can be seen from the individual components of the fit to the electroabsorption spectra in parts c and f of Figure 6 (dashed lines). The fit to the electroabsorption spectrum of the MeTHF sample is of considerably lower quality than the fits to spectra obtained in any of the other matrices. The deviations between the Stark spectrum and the fit for C153 in MeTHF are systematic and have been seen in all data sets obtained. The implications of this result are considered in the discussion section below. Meanwhile, we have summarized the values obtained from these fits for $|\Delta\underline{\mu}|$ and $\overline{\Delta\underline{\underline{\alpha}}}^{\text{Stark}}$ in Table 2. We find the values for $\overline{\Delta\underline{\underline{\alpha}}}^{\text{Stark}}$ of C153 in the organic glasses to be similar to that predicted by ab initio calculations. This finding suggests that in organic glasses the dominant contribution to $\overline{\Delta\underline{\underline{\alpha}}}^{\text{Stark}}$ is that due to $\overline{\Delta\underline{\underline{\alpha}}}^{\text{el}}$.

Dipole Moments and Polarity. In general our measured values of $|\Delta\underline{\mu}|$ for C153 are on the low end of the range of those reported in the literature using various experimental methods (Table 1).[2−7] Our results agree best with that obtained by Marcus and co-workers[7] from their analysis of the steady-state emission spectrum of C153 in which the effects of solute ground-state polarizability are included ($|\Delta\underline{\mu}| \approx 5.0$ D). In contrast, the nonpolarizable solute model predicts a $|\Delta\underline{\mu}|$ of ∼6.0 D.[5] In both cases, these authors used a cavity radius of 3.9 Å, which is appropriate for the "bare" molecular volume of C153. Our results also agree with those of Maroncelli and co-workers[4] who found a value of 4.1 D for $|\Delta\underline{\mu}|$ by modeling their solvatochromic results also using a spherical cavity of radius 3.9 Å.[43] However, when these authors reanalyzed their data by increasing the radius of the cavity by 50% to accommodate C153 plus a contribution from the surrounding solvent shell, the resulting $|\Delta\underline{\mu}|$ increased to ∼7.5 D.[4] This reflects the well-known sensitivity of reaction-field and cavity-field corrections to cavity size. In addition, our results for $|\Delta\underline{\mu}|$ are ∼30% lower than those of Baumann and Nagy[2] and those of Smirnov and Braun.[3] This may possibly be traced to differences in the manner in which the data were analyzed and/or to the fact that our samples were contained in polymers and frozen solvents while these authors made their measurements in the solution phase.

Comparing to the published calculations of $|\Delta\underline{\mu}|$ presented in Table 1, we see that the values measured in this work are in

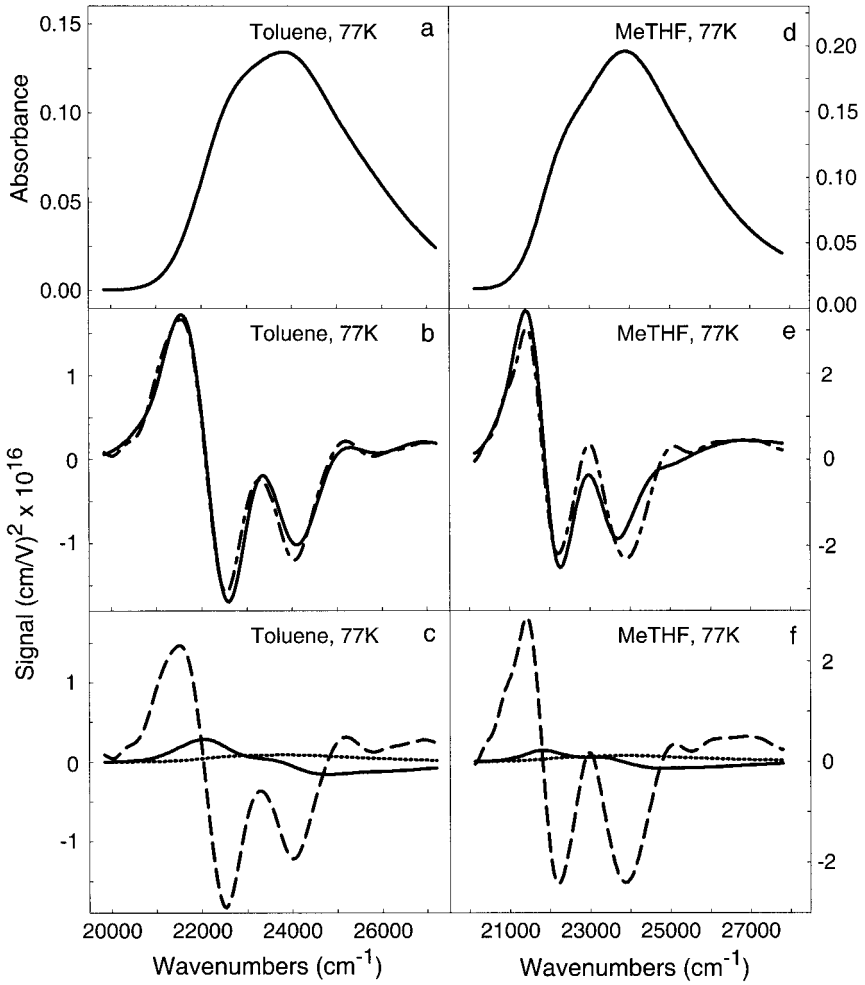

Figure 6. C153 at 77 K in toluene (a−c) and 2-MeTHF (d−f) frozen glasses. The first panel shows the absorption spectrum in toluene (a) and MeTHF (d). The second panel shows the electroabsorption (solid) and fit (dashed−dot) for $\chi = 54.7°$ in toluene (b) and MeTHF (e), respectively. The third panel shows the individual components of the fit to the electroabsorption signal in toluene (c) and MeTHF (f). The absorption spectrum (dotted), first derivative of the absorption spectrum (solid), and the second derivative of the absorption spectrum (dashed), all normalized to the applied field, are shown.

reasonable agreement only with those calculated by ab initio methods.[10] We find that, with the exception of room-temperature PE (vide infra), the increase of $|\Delta\underline{\mu}|$ with ϵ_0 predicted for the calculated values (Table 2) matches that observed quite well, both being ∼25%. This is evidence that the magnitude of the induced moment contribution to $|\Delta\underline{\mu}|$ is rather small within the range of matrix polarities explored here. A small induced moment is consistent with the relatively small values of $\overline{\Delta\underline{\underline{\alpha}}}$ that are calculated and those measured in the low-temperature glasses. Baumann and Nagy also observed a weak dependence of the magnitude of $\overline{\Delta\underline{\underline{\alpha}}}$ on polarity in their solution-phase Stark measurements and estimated a small excited-state polarizability for C153.[2]

Concerning measurements of $|\Delta\underline{\mu}|$, the one somewhat anomalous result we find is that cooling of the PE matrix to below its T_g leads to an increase in the value of $|\Delta\underline{\mu}|$ of C153 from 4.4 to 5.3 D. Note that cooling the PE therefore brings *both* the values of $|\Delta\underline{\mu}|$ and $\overline{\Delta\underline{\underline{\alpha}}}^{\text{Stark}}$ into better agreement with those found in the high-T_g polymers and with calculation. Similarly, decreasing the temperature of the PVC matrix *also* decreased the measured $\overline{\Delta\underline{\underline{\alpha}}}^{\text{Stark}}$ and increased the measured $|\Delta\underline{\mu}|$, though the effect on $|\Delta\underline{\mu}|$ of cooling PVC is less dramatic than that for PE. This explanation for the observed temperature dependencies, which is also detailed in ref 23, is outlined below in the section entitled Orientational Model.

Correlation of Absorption Maxima with Polarity. The absorption maxima of C153 in the various matrices used has also been summarized in Table 2. On the basis of these results, we can make the following three observations. First, the absorption maximum (λ_{max}) of C153 in MeTHF and toluene glasses (418 nm) is shifted ∼10 nm to longer wavelengths from the corresponding room-temperature solution values, suggesting an increase in polarity on freezing with polar solutes.[29] In addition, the λ_{max} of C153 in the room-temperature polymer glasses, PMMA and PVC, is *also* substantially red-shifted from that in room-temperature organic solvents of comparable bulk dielectric constants ($\epsilon_0 \approx 3.5$).[5] This again points to an increase in the local polarity of the probe environment in the glassy state, this time in the polymer glasses. In contrast, the λ_{max} is *not* altered either by lowering the temperature (PVC) or by removing residual solvent and annealing (PMMA). The λ_{max} of C153 in PE (397 nm) is roughly the same as that in solvents of comparable polarity such as cyclohexane ($\epsilon_0 = 2.05$).[5] Moreover, the λ_{max} of C153 in PE is essentially unchanged above and below the T_g of the polymer. Therefore, the PE environment does *not* appear to have an anomalous polarity, at least when C153 is used as the probe.[23]

To rationalize the shifts in the λ_{max} of C153 described above, we can introduce the concept of effective polarity. Effective polarity is the polarity of the local environment containing a

probe molecule within a solid matrix. It may or may not be distinct from the bulk polarity that is defined by ϵ_0 or the empirical solvent parameter π^*.[44,45] The effective polarity of a matrix is that of the solvent in which the probe has the same λ_{max} as it does in the matrix. Comparing the λ_{max}'s measured here to those of Maroncelli et al.,[4] we find that the low-temperature organic glasses and the room-temperature polymer glasses all have very high effective polarities. In fact, it appears that they lie somewhere between those of benzonitrile ($\epsilon_0 = 25.2$) and *N*-methylformamide ($\epsilon_0 = 111$). We can refine this estimate somewhat by noting that the π^* scale is a very good predictor of the solvation behavior of C153.[4,46] By use of this scale, the "effective π^*" of the PMMA, toluene, and MeTHF matrices are ~0.88 while that of PVC is ~0.98. In contrast, the room-temperature π^* of toluene is 0.55 with that of MeTHF expected to be similar.[47] PE, on the other hand, is best described as a medium with a π^* of 0 to 0.18 at both 298 and 77 K, since its λ_{max} is comparable to that of cyclohexane (395 nm).[5]

A model to understand the apparent increase in effective polarity that accompanies freezing of an organic solvent glass was put forward by Bublitz and Boxer.[29] In essence, these authors attribute the increased polarity to a freezing in of the local ordering of the ground-state dipoles or polar groups of the solvent around a solute dipole. The result is an increase in the internal field around the solute that is greater than what would be predicted by the temperature dependence of ϵ_0. Moreover, the magnitude of the effect depends on the $\underline{\mu}_g$ of the probe molecule itself. An increase in the local field causes a shift of the λ_{max} of the solute to lower energies if $\underline{\mu}_e$ is larger than and approximately parallel to $\underline{\mu}_g$ because of the greater stabilization of $\underline{\mu}_e$ relative to $\underline{\mu}_g$. In the context of this model, the red shift of the λ_{max} of C153 in frozen toluene and MeTHF relative to the solution-phase values may be understood. The fact that both solvents shift the λ_{max} of C153 *identically* when frozen may be correlated to the similarity of their bulk solution-phase π^* values.

It may be possible to extend this model to describe the apparent enhancement of the local field in the high-T_g polymers described above. If so, the model would imply that alignment of the pendant groups of the polymer around the ground-state dipoles of C153 is frozen in after the sample is heated to remove the solvent, and the polymer glass is formed. Such an effect is not apparent upon cooling the PE matrix presumably because of the lower polarity of the C−H bonds of this matrix relative to the ester groups of PMMA and the C−Cl bonds of PVC.

In light of the foregoing discussion, one might expect the enhanced local fields of the solid matrices to increase the values of $|\Delta\underline{\mu}|$ and $\overline{\Delta\underline{\underline{\alpha}}}^{Stark}$ of C153 obtained in our experiments relative to those measured in solution phase.[2−7] However, the opposite is the case, at least for $|\Delta\underline{\mu}|$. In addition, the total variation of our measured $|\Delta\underline{\mu}|$ with matrix polarity is ~30%, except for the room-temperature PE results (vide infra). This is similar to the variation in the predicted values that is seen when the cavity and reaction fields are calculated using the *bulk* room-temperature dielectric constants. The resolution of this apparent paradox lies in the fact that for a molecule such as C153 increasing the ϵ_0 of the environment from 2.3 up to a value of 30 only increases the predicted $|\Delta\underline{\mu}|$ from 6.6 to 7.6 D using our calculated results and from 5.0 to 6.2 D using those of ref 10. This increase is less than 25%, which is a much smaller effect than that exhibited by other probes such as cyanine dyes. The reason for this difference in behavior is likely to be that, unlike the cyanine dyes, the ground-state structure of C153 is expected to be relatively invariant to the polarity of its environment.[48]

In contrast to what is found for $|\Delta\underline{\mu}|$, the measured value of $\overline{\Delta\underline{\underline{\alpha}}}^{Stark}$ of C153 varies by nearly 2 orders of magnitude across the range of matrices used. Even though an increased local field will affect the magnitude of $\overline{\Delta\underline{\underline{\alpha}}}^{Stark}$ more than that of $|\Delta\underline{\mu}|$ because the value of $\overline{\Delta\underline{\underline{\alpha}}}^{Stark}$ is proportional to the local field squared while $|\Delta\underline{\mu}|$ scales linearly, the variation observed is clearly larger than could be explained by an enhanced local field. It is therefore evident that polarity is *not* the dominant factor in the value of $\overline{\Delta\underline{\underline{\alpha}}}^{Stark}$ obtained. In the section that follows, we will explore the role played by matrix rigidity in determining the magnitude of $\overline{\Delta\underline{\underline{\alpha}}}^{Stark}$.

Orientational Model. To briefly summarize the relevant electroabsorption results, (1) the measured value of $\overline{\Delta\underline{\underline{\alpha}}}^{Stark}$ for C153 does not vary considerably with polarity, (2) the $\overline{\Delta\underline{\underline{\alpha}}}^{Stark}$'s obtained at 77 K (less than 10 Å^3) agree well with the calculated $\overline{\Delta\underline{\underline{\alpha}}}^{el}$ values, while several of those measured in polymer matrices do *not*, and (3) the increase in $|\Delta\underline{\mu}|$ observed with increasing polarity of the matrix is modest, in agreement with the small calculated $\overline{\Delta\underline{\underline{\alpha}}}^{el}$'s. Here, we will describe our model to explain the observed phenomena. We focus first on the two most anomalous measurements of $\overline{\Delta\underline{\underline{\alpha}}}^{Stark}$, that in room-temperature PE and that in glued PMMA samples. Glued PMMA refers to samples prepared in which the PMMA glass is formed by evaporation of residual dichloroethane. Heated PMMA refers to samples for which the residual solvent is removed by heating (annealing) at 150 °C (see Experimental Section for details).

In the case of C153 in room-temperature PE, lowering the temperature of the matrix brought the measured values better in line with calculation. For glued PMMA samples, the same effect was achieved by removal of the residual solvent through heating and then cooling of the matrix back to room temperature to perform the Stark measurements. At the same time, neither cooling of the PE nor annealing the PMMA appreciably alters the λ_{max}'s of C153 in these matrices, suggesting that the polarity of the C153 environment remains unchanged. Moreover, it is difficult to envision a mechanism whereby the $\overline{\Delta\underline{\underline{\alpha}}}$ of a molecule would vary by orders of magnitude because of polarity while the $|\Delta\underline{\mu}|$ would not. Here, we argue that the variation we observe primarily in $\overline{\Delta\underline{\underline{\alpha}}}^{Stark}$ is correlated most strongly to the *rigidity* of the matrix environment. We will describe first how the electroabsorption measurements are affected by matrix rigidity and then discuss the specifics of the PE and PMMA environments. The mechanism we describe here is elaborated further in ref 23, which is an electroabsorption study of all-trans retinal in various polymer and organic glass matrices.

Because of its rather large ground-state dipole moment (6.55 D),[1] C153 will have a tendency to orient in the field applied in the Stark experiment unless the matrix is sufficiently rigid to prevent its motion. While complete reorientation of the probe is unlikely, rotations of smaller angles may still occur. If so, for each phase of the applied ac electric field, an anisotropic distribution of ground-state dipoles is created with a larger number oriented with the field than against the field. This is the case so long as the dipoles are able to reorient on the time scale of the applied field (500 Hz) or faster. Molecules in environments where reorientation is much slower will behave as though they are static on the time scale of this measurement (vide infra). Absorption of light will instantaneously create an excited-state dipole, $\underline{\mu}_e$, that, in C153, is larger than and nearly parallel to $\underline{\mu}_g$. Note that no additional reorientation of $\underline{\mu}_e$ due to the applied field is possible in an absorption experiment, in accordance with the Born−Oppenheimer principle. The applied

field will more strongly stabilize $\underline{\mu}_e$ than $\underline{\mu}_g$, resulting in an overall shift of the absorption spectrum to lower energies. This shift due to orientation of $\underline{\mu}_g$ occurs *in addition to* shifts arising from the *electronic* ground and excited-state polarizabilities of the molecule. The red-shift arising from orientational motion will manifest itself as a first-derivative contribution to the line shape and therefore contribute to what is measured as $\overline{\Delta\underline{\underline{\alpha}}}^{\text{Stark}}$. Because the ground-state dipole follows the direction of the field, this effect is independent of field direction or is proportional to the field amplitude squared, as is usual for Stark spectra on isotropic samples.

The effect of an orienting $\underline{\mu}_g$ is accounted for in Liptay's formalism by a term proportional to $\beta\,(1/(kT))$ in the third term in eq 3. Neglect of this term for systems in which the molecules are held rigidly in an isotropic distribution is equivalent to setting $\beta \approx 0$. We note that this configuration is equivalent to a very *high* sample temperature because the dipoles remain randomly oriented even in the presence of an aligning field.

A ball-park estimate of the magnitude of $\overline{\Delta\underline{\underline{\alpha}}}^{\text{Stark}}$ that would result when a molecule such as C153 orients by a small amount because of the action of the Stark field shows that this is the likely source of the large $\overline{\Delta\underline{\underline{\alpha}}}^{\text{Stark}}$'s measured here. Using a $\underline{\mu}_g$ of 6.5 D a $\underline{\mu}_e$ of 12 D, assuming the dipoles to be parallel, and using an applied field of 5×10^5 V/cm, we calculate a ground-state orientational polarizability of $\sim$200 Å^3, assuming a reorientation of $\sim$20°.

We anticipate that orientation of the molecule in the field can also cause a somewhat diminished $|\Delta\underline{\mu}|$ to be measured by Stark spectroscopy, as is seen for C153 in room-temperature PE. This can be understood by realizing that in an electroabsorption experiment of the type described here $|\Delta\underline{\mu}|$ is quantified by measuring the broadening induced by an applied field on a fixed and isotropic distribution of dipoles. If an anisotropic distribution is created because of the applied field, the field-induced broadening is consequently diminished. This is because, if the ground-state dipoles are able to follow the direction of the applied field, fewer dipoles will be oriented against the field (high-energy configuration) than is the case for an isotropic distribution. Therefore, the broadening at the high-energy side of the absorption spectrum that is due to increased destabilization of $\underline{\mu}_e$ relative to $\underline{\mu}_g$ will decrease. The result of a smaller field-induced broadening is a smaller measured $|\Delta\underline{\mu}|$ (see Experimental Section).

The first model, described above, tacitly assumes that the dipoles of the matrix will orient to stabilize the $\underline{\mu}_g$ of the probe, whatever its orientation. However, there are two other possible scenarios to consider, which are that (1) the solute dipole reorients in the field while the matrix dipoles remain fixed and (2) the matrix dipoles reorient in the applied field while the solute dipole remains essentially fixed. The first case is unlikely in that if there is sufficient mobility of the matrix to allow partial orientation of the relatively large C153 molecule, it appears that the matrix dipoles of the organic glasses or the pendant groups of the polymers should *also* be able to partially orient, either in response to the applied field or to the field created by the $\underline{\mu}_g$ of C153.

The second case is one in which the response of the matrix molecules to the applied field is equivalent to an enhancement of the local ϵ_0 of the medium. The result would be an increase in the cavity field at the position of the solute. Microscopically, this enhancement is due to the fact that if the environment is not rigid, the dipoles of the matrix can follow the applied field as well as the dipole field of the C153 molecule as described above. While we might expect the reorientation of the matrix dipoles to be small, particularly in a polymer, the additive effect of numerous dipoles can still be substantial. The orientation of the probe dipoles in response to the Stark field would therefore *amplify* the applied field. The prediction of this model is that the effective values of both $|\Delta\underline{\mu}|$ and $\overline{\Delta\underline{\underline{\alpha}}}^{\text{Stark}}$ would be increased by what is effectively a local polarity effect. Naturally, an enhancement in the local polarity would *also* result if both the C153 molecule and the matrix dipoles align in the field as in first model presented above.

To distinguish between the first and third models presented, we appeal to the earlier discussion of the effects of large effective polarities in the matrices on the measured values of $|\Delta\underline{\mu}|$ and $\overline{\Delta\underline{\underline{\alpha}}}^{\text{Stark}}$. That analysis demonstrated that an increase in local polarity would *not* explain an order of magnitude variation in $\overline{\Delta\underline{\underline{\alpha}}}^{\text{Stark}}$ accompanied by a relatively modest variation in $|\Delta\underline{\mu}|$, such as is seen in our results (Table 2). *For this reason, it appears that the dominant contribution to the large* $\overline{\Delta\underline{\underline{\alpha}}}^{\text{Stark}}$*'s measured in this experiment arises from rotation of the probe molecule induced by the applied field in matrices that are not fully rigid.*

Of all the matrices studied, room-temperature PE is expected to afford the most mobility to the C153 molecules. At room temperature, PE is known to consist of both amorphous and crystalline regions.[49] Dopants such as C153 are thought to reside primarily at the amorphous region or at the interface of the two.[50] Polymers above their T_g, as is PE at 298 K, exhibit fairly large-scale motions of their constituent chains.[51a] For example, dielectric measurements on bulk low-density PE suggest that there is considerable mobility of the polymer chains at 25 °C at the frequencies probed in this experiment ($\sim$500 Hz), though the peak of the dielectric loss curve at this temperature occurs at at a frequency of $\sim$5 Hz.[51b] We therefore expect that considerable mobility of the dopant C153 is *also* possible when the amorphous region of the PE matrix is in its rubbery phase (above T_g). This would result in the large $\overline{\Delta\underline{\underline{\alpha}}}^{\text{Stark}}$ of C153 in room- versus low-temperature PE. A similar effect was also observed by Saal and Haase in studies of a dye doped into PMMA and probed by electroabsorption at a temperature above the T_g of the polymer.[52]

In the case of the glued PMMA samples, it is known that trapped solvents can lower the T_g of a polymer.[53a] We therefore postulate that residual solvents lower the rigidity of the molecular cavity in the region of the C153 molecule. Heating of the polymer may also have the effect of annealing it so that the environment of C153 is consequently more rigid. In addition, orientational motion of the trapped solvent molecules *themselves* may be contributing to the effects we observe. Any one of these effects could explain the observation that the measured $\overline{\Delta\underline{\underline{\alpha}}}^{\text{Stark}}$ of the probe in the heated PMMA is dramatically reduced from that measured in glued PMMA. It is interesting to note that Richert and co-workers have observed a decay in the SHG signal arising from chromophores doped into poly(isobutyl methacrylate) containing residual chloroform, which they attribute to a local field effect.[53b]

Finally, an interesting result of the polymer studies, from the standpoint of nonlinear optical applications, is the observation that mobility of C153 in the high-T_g polymer PVC is *not* completely eliminated until the temperature of the heated (annealed) sample is lowered significantly below room temperature. Therefore, the available thermal energy at 298 K is sufficient to allow some orientation of the probe with the applied field. Such residual mobility is likely to be linked[54a] to the decay over time in the field-induced alignment of molecules within glassy polymers that is produced by corona poling.

Related to this phenomenon, the decay of photoinduced orientation of dyes in PMMA and other high-T_g polymers has been measured by Dumont and co-workers who found a hierarchy of relaxation times from nearly instantaneous to those occurring over the course of a week.[54b] These results suggest that a polymer sample is highly heterogeneous with respect to the mobility of dye molecules embedded in it. While the description of the model presented above to explain the results of our experiments implies a more homogeneous distribution of relaxation times, this is by no means a necessary feature. We emphasize that our measurements are specifically sensitive to reorientation on the time scale of the applied field (~500 Hz) and may be probing a subset of molecules that can respond to a field fluctuating on that time scale. If the frequency of the field were to be substantially increased, the expected result would be that most of the molecules would no longer be able to follow the field and would behave as though they are in a "rigid" environment from the standpoint of their response to the Stark field. Lowering the frequency of the field would increase the likelihood that even molecules in relatively rigid environments could reorient in response. This is what was observed in the measurements of Saal and Haase.[52] Experiments to explore this effect in the systems studied here are currently underway.

Heterogeneity in the Electroabsorption Spectrum. The fits to the electroabsorption spectra described above allow us to address a point debated in the literature regarding whether there are multiple underlying electronic states underlying the main absorption band of C153. To briefly summarize, C153 has for many years been thought to be a nonspecific probe of solvation dynamics. This implies that excitation anywhere within the absorption band populates a single excited state and that subsequent shifts in the fluorescence maximum of the molecule reflect *only* the dynamics of the solvent response to its dipole moment (μ_e) and *not* relaxation between excited vibrational and/or electronic levels. One experimental observation that argues against this model is the observed dependence of the emission decay curves on excitation wavelength. While several arguments have been put forward in the literature to explain this phenomenon,[55,56] the one we will focus on here is that due to Blanchard and co-workers.[41,57] Semiempirical calculations by these authors showed the presence of two distinct electronic states within the absorption envelope of C153, S_1 and S_2, having excited-state dipole moments of 11 and 8.4 D, respectively.[41] In the model, the minimum of the S_1 potential energy well is more strongly displaced than that of S_2 from the minimum of the ground-state surface. Therefore, excitation on the low-energy side of the absorption band (410−430 nm) populates a mixture of S_1 and S_2 while excitation on the high-energy side mostly populates S_1 (350−390 nm). As a result, effects due to S_2 should be most apparent on the low-energy side of the electroabsorption spectrum while those due to S_1 will be more obvious on the high-energy side, even though the calculated energy separation between the two excited states is small (~600 cm^{-1}).[41]

It has been observed that inhomogeneity in the electronic properties of the molecule, such as that described above, manifests itself as a very poor-quality fit to the electroabsorption spectrum if a single set of fitting coefficients (a_χ, b_χ, c_χ) is used.[58−61] This is because the shift and broadening of the absorption spectrum (due to $|\Delta\underline{\mu}|$ and $\overline{\Delta\underline{\underline{\alpha}}}^{Stark}$) needed to reproduce the Stark spectrum will not be uniform across the wavelength region probed. In contrast, for all but one of the matrices studied here, a high-quality fit to the Stark spectrum was obtained using simple derivatives of the absorption spectrum. The exception, C153 in MeTHF, will be discussed in more detail below. Moreover, the quality of that fit is not strongly dependent on the polarity of the matrix. Such variability might be predicted on the basis of the model described above, since the relative energies of S_1 and S_2 should be polarity-dependent. *Therefore, the majority of these data are more consistent with the conclusion that the absorption band of C153 consists of a single optically allowed transition.*

The relatively poor fit to the electroabsorption spectrum of C153 in MeTHF suggests that inhomogeneity in the absorption spectrum can arise in some environments. We attempted to improve the quality of the fit by deconvolving the absorption band into individual Gaussian bands that would represent its underlying vibronic or electronic states. An improvement in the fit was obtained using a minimum of two bands. However, no physically meaningful parameters could be derived from the fit because of the extensive overlap of the Gaussians used. Therefore, though there is strong evidence for inhomogeneity in the absorption spectrum of C153 in frozen MeTHF, we cannot conclusively state whether it arises from the presence of multiple electronic states.[41]

Conclusions

The calculated values of $\overline{\Delta\underline{\underline{\alpha}}}^{el}$ for C153 and the measured values of $\overline{\Delta\underline{\underline{\alpha}}}^{Stark}$ agree, both being less than 10 $Å^3$, when the matrix containing the probe molecule is rigid. In nonrigid matrices, the orientational contribution to $\overline{\Delta\underline{\underline{\alpha}}}^{Stark}$ can be several hundreds of $Å^3$. Therefore, Stark spectroscopy is a sensitive probe of molecular motion, even in polymers that are below their glass-transition temperatures.

Acknowledgment. We thank Dr. David Yaron and Dr. Hyung Kim for useful discussions, Dr. Zhigang Shuai for INDO/SCI/SOS calculations on C153, and Dr. Marshall Newton for ab initio (6-21G*) results on C153. We acknowledge our sources of funding, The NSF-CAREER and POWRE programs, and the Center for Molecular Analysis at Carnegie Mellon University for the use of the absorption spectrometer. The calculations were performed on a Pentium II computer donated by Intel, Inc. as part of the "Technology for Education 2000" initiative.

References and Notes

(1) Moylan, C. *J. Phys. Chem.* **1994**, *98*, 13513.
(2) Baumann, W.; Nagy, Z. *Pure Appl. Chem.* **1993**, *65*, 1729. For a reference containing electrooptical measurements on other coumarin dyes, see Nemkovich, N. A.; Reis, H.; Baumann, W. *J. Lumin.* **1997**, *71*, 255.
(3) Smirnov, S. N.; Braun, C. L. *Rev. Sci. Instrum.* **1998**, *69*, 2875.
(4) Horng, M. L.; Gardecki, J. A.; Papazyan, A.; Maroncelli, M. *J. Phys. Chem.* **1995**, *99*, 17311.
(5) Maroncelli, M.; Fleming, G. R. *J. Chem. Phys.* **1987**, *86*, 6221.
(6) Rechthaler, K.; Kohler, G. *Chem. Phys.* **1994**, *189*, 99.
(7) Hsu, C.-P.; Georgievskii, Y.; Marcus, R. A. *J. Phys. Chem. A* **1998**, *102*, 2658.
(8) McCarthy, P. K.; Blanchard, G. J. *J. Phys. Chem.* **1993**, *97*, 12205.
(9) Cichos, F.; Brown, R.; Rempel, U.; Borczyskowski, C. v. *J. Phys. Chem. A* **1999**, *103*, 2506.
(10) Newton, M. Personal communication.
(11) Oudar, J. L. *J. Chem. Phys.* **1977**, *67*, 446.
(12) Kumar, P. V.; Maroncelli, M. *J. Chem. Phys.* **1995**, *103*, 3038.
(13) Ando, K. *J. Chem. Phys.* **1997**, *107*, 4585.
(14) Muino, P.; Callis, P. *J. Chem. Phys.* **1994**, *100*, 4093.
(15) Bursulaya, B.; Kim, H. J. *J. Phys. Chem.* **1996**, *100*, 16451.
(16) Bursulaya, B. D.; Zichi, D. A.; Kim, H. J. *J. Phys. Chem.* **1995**, *99*, 10069.
(17) Bursulaya, B. D.; Zichi, D. A.; Kim, H. J. *J. Phys. Chem.* **1996**, *100*, 1392.
(18) Matyushov, D. V.; Voth, G. A. *J. Phys. Chem.*, submitted.
(19) Liptay, W. In *Modern Quantum Chemistry Part III: Action of Light and Organic Crystals*; Sinanoglu, O., Ed.; Academic Press: New York, 1965; p 45.

(20) Bublitz, G. U.; Boxer, S. G. *Ann. Rev. Phys. Chem.* **1997**, *48*, 213.
(21) Locknar, S. A.; Peteanu, L. A. *J. Phys. Chem. B* **1997**, *102*, 4240.
(22) Locknar, S. A.; Peteanu, L. A.; Shuai, Z. *J. Phys. Chem. A* **1999**, *103*, 2197.
(23) Locknar, S. A.; Chowdhury, A.; Peteanu, L. A. Submitted for publication.
(24) Tallent, J. R.; Birge, J. R.; Zhang, C.-F.; Wenderholm, E.; Birge, R. R. *Photochem. Photobiol.* **1992**, *56*, 935.
(25) Marder, S. R.; Perry, J. W.; Bourhill, G.; Gorman, C. B.; Tiemann, B. G.; Mansour, K. *Science* **1993**, *261*, 186.
(26) Hudson, B. S.; Kohler, B. E. *J. Chem. Phys.* **1973**, *59*, 4984.
(27) Hug, G.; Becker, R. S. *J. Chem. Phys.* **1976**, *65*, 55.
(28) Lewis, J. E.; Maroncelli, M. *Chem. Phys. Lett.* **1998**, *282*, 197.
(29) Bublitz, G. U.; Boxer, S. G. *J. Am. Chem. Soc.* **1998**, *120*, 3988.
(30) Bublitz, G. U.; Ortiz, R.; Runser, C.; Fort, A.; Barzoukas, M.; Marder, S. R.; Boxer, S. G. *J. Am. Chem. Soc.* **1997**, *119*, 2311.
(31) Liptay, W. In *Excited States*; Lim, E. C., Ed.; Academic Press: New York, 1974; p 128.
(32) Liptay, W. *Angew. Chem., Int. Ed. Engl.* **1969**, *8*, 177.
(33) Rohlfing, F.; Bradley, D. D. C. *Chem. Phys. Lett.* **1997**, *277*, 406.
(34) Frisch, M. J.; Trucks, G. W.; Schlegel, H. B.; Gill, P. M. W.; Johnson, B. G.; Robb, M. A.; Cheeseman, J. R.; Keith, T.; Peterson, G. A.; Montgomery, J. A.; Raghavachari, K.; Al-Laham, M. A.; Zakrzewski, V. G.; Ortiz, J. V.; Foresman, J. B.; Cioslowski, J.; Stefanov, B. B.; Nanayakkara, A.; Challacombe, M.; Peng, C. Y.; Ayala, P. Y.; Chen, W.; Wong, M. W.; Andres, J. L.; Repogle, E. S.; Gomberts, R.; Martin, R. L.; Fox, D. J.; Binkley, J. S.; Defrees, D. J.; Baker, J.; Stewart, J. P.; Head-Gordon, M.; Gonzales, C.; Pople, J. A. *Gaussian 94*, revision E.2; Gaussian, Inc.: Pittsburgh, PA, 1995.
(35) Mathies, R.; Albrecht, A. C. *J. Chem. Phys.* **1974**, *60*, 2500.
(36) Shuai, Z.; Beljonne, D.; Brédas, J.-L. *J. Chem. Phys.* **1992**, *97*, 1132.
(37) Shuai, Z. Personal communication.
(38) Premvardhan, L.; Peteanu, L. *Chem. Phys. Lett.* **1998**, *296*, 521.
(39) Bottcher, C. J. F. *Theory of Electric Polarisation*; Elsevier Publishing Co.: Amsterdam, 1952.
(40) Richert, R. *Chem. Phys. Lett.* **1993**, *216*, 223.
(41) Jiang, Y.; McCarthy, P. K.; Blanchard, G. J. *Chem. Phys.* **1994**, *183*, 249.
(42) Rössler, E.; Sillescu, H. *Chem. Phys. Lett.* **1984**, *112*, 94.
(43) The experimental numbers reported here contain both the reaction field and cavity field components. Therefore in the case of C153, the corresponding gas-phase values for $|\Delta\underline{\mu}|$ and $\Delta\underline{\underline{\alpha}}$ would actually be somewhat lower than those reported in Table 2. Since the calculated values are reaction-field- and cavity-field-corrected, one can compare those in Table 2 to the calculated gas-phase values (Experimental Section) to estimate the cavity-field and reaction-field contributions to $|\Delta\underline{\mu}|$ and $\Delta\underline{\underline{\alpha}}$ that would be predicted by the dielectric continuum model.
(44) Kamlet, M. J.; Abboud, J. L.; Taft, R. W. *J. Am. Chem. Soc.* **1977**, *99*, 6027.
(45) Laurence, C.; Nicolet, P.; Dalati, M. T.; Abboud, J.-L. M.; Notario, R. *J. Phys. Chem.* **1994**, *98*, 5807.
(46) Moog, R. S.; Davis, W. W.; Ostrowski, S. G.; Wilson, G. L. *Chem. Phys. Lett.* **1999**, *299*, 265.
(47) The values of π^* for THF and toluene are 0.55 and 0.49, respectively. While MeTHF may be expected to have a different value of π^* than THF, addition of a methyl group causes a decrease of 0.06 units between benzene and toluene. If a similar decrease occurs in THF, this would make the π^* values of MeTHF and toluene similar at room temperature.
(48) Marder, S. R.; Perry, J. W.; Tiemann, B. G.; Gorman, C. B.; Gilmour, S.; Biddle, S. L.; Bourhill, G. *J. Am. Chem. Soc.* **1993**, *115*, 2524.
(49) Bovey, F. A. *Chain Structure and Conformation of Macromolecules*; Academic Press: New York, 1982.
(50) Zimmerman, O. E.; Weiss, R. G. *J. Phys. Chem. A* **1998**, *102*, 5364.
(51) (a) Rössler, E. *Phys. Rev. Lett.* **1990**, *65*, 1595. (b) Graff, M. S.; Boyd, R. H. *Polymer* **1994**, *35*, 1797.
(52) Saal, S.; Haase, W. *Chem. Phys. Lett.* **1997**, *278*, 127.
(53) (a) Van Krevelen, D. W. *Properties of Polymers*; Elsevier: Amsterdam, 1997. (b) Shüssler, S.; Albrecht, U.; Richert, R.; Bässler, H. *Macromolecules* **1996**, *29*, 1226.
(54) (a) Dhinojwala, A.; Wong, G. W.; Torkelson, J. M. *Macromolecules* **1993**, *26*, 5943 and references therein. (b) El Osman, A.; Dumont, M. *Polym. Prepr., Am. Chem. Soc. Div. Polym. Chem.* **1998**, *39*, 300.
(55) Agmon, N. *J. Phys. Chem.* **1990**, *94*, 2959.
(56) Maroncelli, M.; Fee, R. S.; Chapman, C. F.; Fleming, G. R. *J. Phys. Chem.* **1991**, *95*, 1012.
(57) Flory, W. C.; Blanchard, G. J. *Appl. Spectrosc.* **1998**, *52*, 82.
(58) Premvardhan, L.; Peteanu, L. *J. Phys. Chem. A* **1999**, *103*, 7506.
(59) Liptay, W.; Wortmann, R.; Bohm, R.; Detzer, N. *Chem. Phys.* **1988**, *120*, 439.
(60) Reimers, J.; Hush, N. S. *J. Phys. Chem.* **1991**, *95*, 9773.
(61) Pierce, D. W.; Boxer, S. G. *Biophys. J.* **1995**, *68*, 1583.
(62) Lide, D. R. *Handbook of Chemistry and Physics*; CRC Press: Boca Raton, FL, 1998.